JACS
JOURNAL OF THE AMERICAN CHEMICAL SOCIETY
Article
pubs.acs.org/JACS

Understanding Intrinsically Irreversible, Non-Nernstian, Two-Electron Redox Processes: A Combined Experimental and Computational Study of the Electrochemical Activation of Platinum(IV) Antitumor Prodrugs

Meghan C. McCormick,[†] Karlijn Keijzer,[†] Abhigna Polavarapu,[†] Franklin A. Schultz,[†,‡] and Mu-Hyun Baik*[,†,§]

[†]Department of Chemistry, Indiana University, 800 East Kirkwood Avenue, Bloomington, Indiana 47405, United States
[‡]Department of Chemistry, Indiana University-Purdue University Indianapolis, 402 North Blackford Street, Indianapolis, Indiana 46202, United States
[§]Department of Chemistry, Korea University, 208 Seochang, Chochiwon, Chung-nam 339-700, South Korea

Supporting Information

ABSTRACT: Six-coordinate Pt(IV)-complexes are prominent prodrug candidates for the treatment of various cancers where, upon two-electron reduction and loss of two axial ligands, they form more familiar, pharmacologically active four-coordinate Pt(II) drugs. A series of electrochemical experiments coupled with extensive density functional calculations has been employed to elucidate the mechanism for the two-electron reduction of $Pt^{IV}(NH_3)_2Cl_2L_2$ to $Pt^{II}(NH_3)_2Cl_2$ (L = CH_3COO^-, **1**; L = $CHCl_2COO^-$, **2**; L = Cl^-, **3**). A reliable estimate for the normal reduction potential E^o is derived for the electrochemically irreversible Pt(IV) reduction and is compared directly to the quantum chemically calculated reduction potentials. The process of electron transfer and Pt−L bond cleavage is found to occur in a stepwise fashion, suggesting that a metastable six-coordinate Pt(III) intermediate is formed upon addition of a single electron, and the loss of both axial ligands is associated with the second electron transfer. The quantum chemically calculated reduction potentials are in excellent agreement with experimentally determined values that are notably more positive than peak potentials reported previously for **1**−**3**.

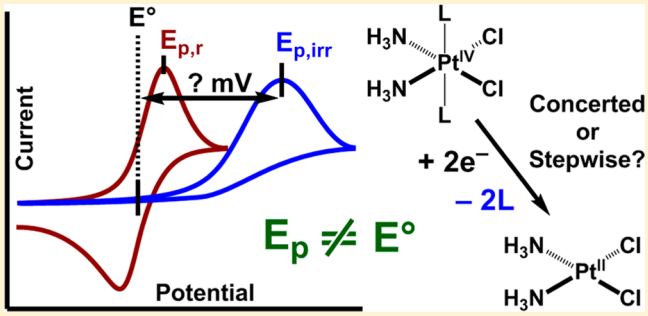

INTRODUCTION

Platinum-based antitumor drugs continue to play an important role in the treatment of various cancers, including testicular, head and neck cancers, and ovarian and lung carcinomas.[1−5] Unfortunately, serious side effects, such as nephrotoxicity and neurotoxicity, and resistance to the first generation of Pt drugs pose severe limitation to their efficacy.[6−9] One promising avenue of decreasing side effects is to utilize much more inert six-coordinate Pt(IV) prodrugs that will be reduced once inside the target cell to afford the active, four-coordinate, square-planar Pt(II) analogues.[10−17] Much work has been invested to elucidate the manner in which cisplatin, $Pt^{II}(NH_3)_2Cl_2$, binds to DNA;[18−24] therefore, a rational strategy for designing Pt(IV)-prodrugs is to incorporate a cisplatin moiety into a Pt(IV)-complex with axial ligands that will be lost upon reduction.[13,14,25−28] Furthermore, the choice of the axial ligands employed can be made on the basis of tunable properties, such as lipophilicity[29−31] or ease of reduction.[14,29,30,32−36] The activation process involving the transfer of two electrons and loss of two axial ligands is challenging to study, in part because the reduction is intrinsically irreversible, making it difficult to use standard voltammetric methods to precisely characterize the redox properties of the Pt(IV/II) couple. In addition, the two-electron redox process, which is commonly observed as a single voltammetric event, complicates the conceptual understanding.[34] Finally, the thermodynamics and kinetics of the overall dissociative electron-transfer process can be influenced greatly by the timing of the axial bond cleavage. Because no straightforward solutions exist for these complications, previous studies utilized the peak potential of the irreversible cathodic response, E_{pc}, at a single scan rate to approximate the ease of reduction of the complex.[13,29,30,32−34,37] These studies have provided some valuable insight, but the peak potential of an irreversible redox reaction is highly dependent on the scan rate and other experimental conditions, posing serious questions about the relevance of these potentials for understanding the redox behavior of the Pt(IV) drugs. In addition, the physical

Received: March 24, 2014
Published: May 22, 2014

   dx.doi.org/10.1021/ja5029765 | J. Am. Chem. Soc. 2014, 136, 8992−9000

meaning of the two-electron wave remains obscure when the extent of coupling between the underlying electrochemical and chemical steps within the time scale of the measurement is not known.

A much better, albeit more involved method of inquiry is to quantify the energetics of electron transfer and Pt−L bond cleavage within the framework of Marcus theory.[38] Savéant[39−47] has developed a powerful conceptual approach for characterizing such dissociative electron transfer reactions. The analysis utilizes the peak potential, the shape of the $i-E$ response, and the scan rate dependence of these parameters to extract the electron transfer coefficient α. The value of α and its variation with scan rate contain valuable information about the redox mechanism and allow for identifying whether the chemical step of bond cleavage and electron transfer are stepwise or concerted processes. As an additional benefit, the standard reduction potential E^{o}, which has been inaccessible thus far for Pt(IV) prodrugs, can be extracted. Although Savéant's analysis has been used mainly for organic systems to date,[39−47] there is no fundamental reason why it should not be fully applicable to transition-metal complexes. The emerging mechanistic insight from these studies can be significantly enhanced by augmenting them with detailed quantum chemical models. This combination allows for constructing an unprecedentedly precise model for the overall redox reaction, including a quantitative interpretation of the single two-electron response and projections for the behavior of the Pt(IV) prodrugs in biological environments.

Over the past decade, we have demonstrated that density functional theory (DFT) combined with continuum solvation models constitutes a sufficiently accurate model for evaluating the energies of even complex redox processes,[48−52] with redox potentials being reproduced within ∼100 mV. Typically, these calculations assume Nernstian behavior of the redox pairs and only afford standard potentials, because they do not provide any information about the kinetics of electron transfer or the existence of metastable intermediates. The strengths of this computational electrochemistry approach are that it allows for examining the electronic structure of the redox intermediates in detail and it is complementary to the experimental explorations presented here. As these calculations simply locate redox intermediates, the methodology is not limited to Nernstian redox couples per se. It should be possible to employ the same modeling techniques to non-Nernstian behavior, provided that the kinetic information leading to deviations from standard equilibrium thermodynamics is taken from a different means, in this case from experiments. Here, we demonstrate such an extension to redox chemistry modeling by combining our DFT calculations with the aforementioned Savéant analysis.

EXPERIMENTAL AND COMPUTATIONAL DETAILS

Synthesis of Complexes. The platinum prodrugs **1**−**3** were generously provided by Professor Stephen J. Lippard (Massachusetts Institute of Technology, Cambridge, MA). The general procedures for the synthesis of these prodrugs have been reported previously elsewhere.[27,34]

Computational Details. All calculations were carried out using density functional theory as implemented in the Jaguar 7.0 suite[53] of *ab initio* quantum chemistry programs. Geometry optimizations were performed using the B3LYP[54−57] functional and the 6-31G** basis set. Pt was represented using the Los Alamos LACVP basis[58,59] which includes relativistic effective core potentials. The energies of the optimized structures were reevaluated by additional single-point energy calculations of each optimized geometry using Dunning's correlation consistent triple-ζ basis set[60] cc-pVTZ(-f) that includes a double set of polarization functions. For Pt, a modified version of LACVP was used, designated as LACV3P, in which the exponents were decontracted to match the effective core potentials with triple-ζ quality. Solvation energies were evaluated using a self-consistent reaction field (SCRF) approach based on accurate numerical solutions of the Poisson−Boltzmann equation.[61−63] Solvation calculations were carried out with the 6-31G**/LACVP basis at the optimized gas-phase geometry employing a dielectric constant of ε = 80.37 for water. For all continuum models, the solvation energies are subject to empirical parametrization of the atomic radii which are used to generate the solute surface. We employed the standard set[64] of optimized radii in Jaguar for H (1.150 Å), C (1.900 Å), O (1.550 Å), N (1.600 Å), Cl (1.974), and Pt (1.377 Å). Analytical vibrational frequencies within the harmonic approximation were computed with the 6-31G**/LACVP basis set to confirm proper convergence to well-defined minima on the potential energy surface. The electron attachment energy in solution, ΔG^{EA}, was calculated by computing the energy components:

$$\Delta G^{EA}(\mathrm{sol}) = \Delta G^{EA}(\mathrm{GP}) + \Delta G^{solv} \quad (1)$$

$$\Delta G^{EA}(\mathrm{GP}) = \Delta H^{EA}(\mathrm{GP}) - T\Delta S(\mathrm{GP}) \quad (2)$$

$$\Delta H^{EA}(\mathrm{GP}) = \Delta E^{EA}(\mathrm{SCF}) + \Delta \mathrm{ZPE} \quad (3)$$

ΔG^{EA}(GP) is the free energy in gas phase; ΔG^{solv} is the free energy of solvation as computed using the continuum solvation model; ΔH^{EA}(GP) is the enthalpy in the gas phase; T is the temperature (298 K); ΔS(GP) is the entropy in the gas phase; ΔE^{EA}(SCF) is the self-consistent field energy, i.e. the "raw" electronic energy as computed from the SCF procedure; and ZPE is the zero-point energy. The ZPE and entropy were retrieved from the vibrational frequency calculation. Note that by entropy we refer specifically to the vibrational/rotational/translational entropy of the solute(s); the entropy of the solvent is incorporated implicitly in the continuum solvation model.

Electrochemistry. Cyclic voltammetry experiments of all Pt(IV) prodrugs were conducted in a three-electrode cell and recorded at room temperature with an EG&G PAR 273A potentiostat. The working electrode was a platinum disk (Bioanalytical Systems, area = 0.02 cm^2) or gold disk (Bioanalytical Systems, area = 0.02 cm^2), the reference electrode was Ag/AgCl (Bioanalytical Systems, satd. NaCl), and the counter electrode was a platinum wire. The potential of the Ag/AgCl electrode is +0.197 V vs SHE. Pt(IV)-complexes were dissolved in water to prepare 1 mM solutions with 0.1 M sodium acetate (for **1** and **2**) or potassium chloride (for **3**) as the supporting electrolyte. Solutions were degassed with Ar for 5−10 min before experimentation, and each CV was collected under a blanket of Ar. The platinum disk electrode was polished between CV trials with 0.05-μm γ-alumina (Buehler) slurry, rinsed clean with DI water, and dried. Scan rates ranging from 0.02 to 1 V s^{-1} were used (0.05 to 1.5 V s^{-1} in the case with gold); three CVs were collected at each scan rate to obtain an average peak potential (Tables S5 and S6 in SI). Experiments began with a CV scan rate of 0.1 V s^{-1} and then were collected at 0.2, 0.5, and 1 V s^{-1}. At this point, another CV was obtained at 0.1 V s^{-1} to check the reproducibility of the system. Subsequently, CVs were collected at 0.05 and 0.02 V s^{-1}. Overall, the peak potentials obtained at 0.1 V s^{-1} did not change significantly (maximum uncertainty of ∼17 mV, shown in Table S5 in SI). All voltammograms were background corrected by numerically subtracting the current obtained for the supporting electrolyte alone from that of the sample solution. Peak potentials were located by fitting a Lorentzian to ∼20 data points close to the maximum current.

RESULTS AND DISCUSSION

The key to understanding the reductive activation of the Pt(IV) prodrug into its Pt(II) form lies in identifying the principal components of the overall reaction and understanding how they are coupled to one another. The electrochemical potential, at which the reductive activation of the prodrug occurs, is

dx.doi.org/10.1021/ja5029765 | J. Am. Chem. Soc. 2014, 136, 8992−9000

determined by the energy required to inject two electrons into the Pt(IV) center and the energetics associated with losing two ligands. The experimentally observable redox properties are therefore complex composites of electrochemical and chemical events and are intimately connected to the mechanistic details of the prodrug activation reaction. Treating the Faradaic response of the Pt(IV)-complex as a simple two-electron transfer can therefore be misleading. Scheme 1 shows a

Scheme 1

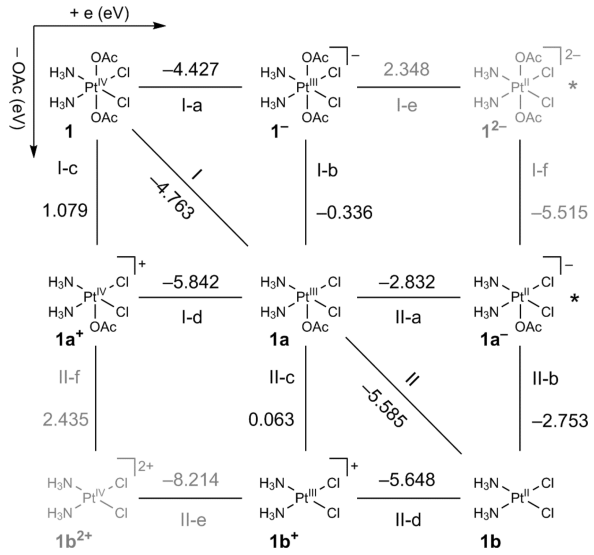

conceptual decomposition of the electron transfer and ligand loss processes. The energetic requirements for each of the components were evaluated quantum chemically by using a computational protocol that was shown to yield reasonably accurate models of solution-phase redox processes in previous work.[49] Starting from the six-coordinate Pt(IV)-complex, we calculated the energy components by first adding an electron but not allowing the axial ligand to depart from the Pt-coordination site and then in a separate calculation reevaluating the energy of the Pt-complex with each of the two axial ligands removed sequentially.[50,65] Scheme 1 shows a visualization of this series of calculations where the electron attachment energies in eV are displayed in the horizontal direction and ligand dissociation energies are given in the vertical direction. The structures denoted with an asterisk indicate that the geometry optimizations of these intermediates, which are necessarily done in the gas phase, resulted in no meaningful minima; more specifically, chemically meaningless structures are obtained where the reduced metal center can no longer hold the anionic ligands in the primary coordination sphere (Figure S1 in SI). Instead, the detached axial ligands form hydrogen bonds with the ammine hydrogens; these minima are plausible in gas phase, but they are not realistic as an approximation to solution-phase structures. As a more reasonable alternative, the energies for these species were obtained from single-point energy calculations of the optimized geometries of their respective Pt(III) analogues (Table S3 in SI).

It is instructive to examine the energies that connect the various hypothetical intermediates in this conceptual scheme. On the basis of electrostatic considerations alone,[48,66,67] one may expect the reduction of Pt(IV) to be easier than that of Pt(III), but given how rare Pt(III)-complexes are[68−71] it is chemically intuitive to expect that the Pt(III)-complex will be easily reduced to the more common Pt(II) form. Our energy decomposition scheme allows for consolidating these seemingly opposing expectations from purely physical and chemically intuitive views: The electron attachment energy is computed to be −4.427 eV (Step I-a) for the six-coordinate Pt(IV)-complex **1**, which is much more favorable than −2.832 eV, obtained for the five-coordinate Pt(III) intermediate at the center of Scheme 1 (Step II-a). These energies are in good agreement with the view that adding an electron to Pt(IV) should be much easier than adding another electron to the resulting Pt(III) center, based on electrostatic arguments alone. The ligand dissociation energies represented by Steps I-b and II-b are dramatically different, however. Loss of the first acetato ligand from the one-electron reduced species $\mathbf{1}^-$ is energetically downhill by 0.336 eV (7.7 kcal mol^{-1}), whereas loss of the second acetato ligand lowers the energy of the Pt(II)-complex by 2.753 eV (63.5 kcal mol^{-1}). These energy components add to give adiabatic reduction energies of −4.763 and −5.585 eV, respectively, which is in good agreement with the chemically intuitive expectation that the putative Pt(III)-complex should be easy to reduce. Thus, our calculations highlight the importance of the disproportionate distribution of the energy associated with the loss of axial ligands when rationalizing the redox instability of Pt(III)—a straightforward relationship that is not always appreciated as clearly as demonstrated in our computational decomposition scheme.

The nonclassical energy ordering where the second reduction is thermodynamically more favorable than the first is commonly referred to as "potential inversion" and gives rise to a single two-electron response in electrochemical measurements.[52,66,72−74] This scenario is readily confirmed by our experimental voltammetric studies where a single, irreversible two-electron reduction is seen, as shown in red in Figure 1 for

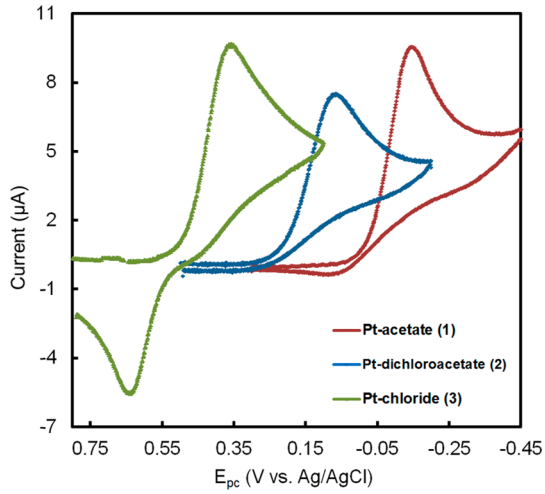

Figure 1. Background subtracted cyclic voltammograms of prodrugs **1**−**3** at 0.1 V s^{-1}.

complex **1**. Our calculations show that the singly reduced, five-coordinate Pt(III) species is electronically stable in that it resides in a proper minimum on the electronic energy surface, but the loss of the acetato ligand is easy to accomplish on the free energy surface, as the translational entropy gain of approximately 10 kcal mol^{-1} associated with the ligand loss compensates for the electronic energy loss associated with the

dx.doi.org/10.1021/ja5029765 | J. Am. Chem. Soc. 2014, 136, 8992−9000

Pt(III)−O bond cleavage resulting in a free energy of ligand dissociation of only 1.5 kcal mol^{-1} (Step II-c). The most plausible interpretation of such a small energy difference between **1a** and **1b**$^+$ is that species **1a** may irreversibly lose the axial ligand to afford **1b**$^+$ under normal conditions, as the relatively low concentration of the acetate in solution should prevent any equilibrium between **1a** and **1b**$^+$ to be established. This interpretation assumes that the kinetics of ligand loss is fast and does not lead to any metastable intermediates that exist within the lifetime of the electrochemical measurement. The kinetics of losing a negatively charged ligand triggered by electron transfer is difficult to model with currently available quantum chemical methods; however, the dynamics of how solvent interacts explicitly with each of the molecular fragments is key in determining the lifetime of the Pt(III)-intermediate. The acetato ligand may remain close to the Pt-center, taking advantage of the secondary coordination sphere.

A calculation for the extent of potential inversion requires a determination of the most likely intermediate redox state from our conceptual decomposition in Scheme 1. Defining the values of the two redox potentials E_1° and E_2° relies on whether the energy of the ligand loss contributes to the energy of electron transfer; thus, several scenarios could be imagined for which energy values should be involved. E_1° could simply be taken from Step I where loss of the first axial ligand is thermodynamically favored after the initial electron transfer. Conversely, the value of E_2° is complicated by possible involvement of the second ligand loss and its energetic contribution. Energetically, the exact composition of the intermediate redox state preceding E_2° is not important due to the small energy difference between **1a** and **1b**$^+$, i.e. the predicted value of E_2° is nearly identical for both models that differ in the number of ligands bound to the Pt(III)-center. In any case, we can calculate the extent of potential inversion of one plausible scenario by obtaining the energy difference between steps I and II, which suggests that the two redox potentials are inverted by as much as 822 mV. Similar scenarios are seen for complexes **2** and **3** as summarized in Table 1,

Table 1. Energy Decomposition (eV) of the Reduction Process for Compounds 1−3

cmpd	step I	step II	ΔE
1	−4.763	−5.585	−0.822
2	−5.224	−5.820	−0.596
3	−4.936	−5.500	−0.564

where the reduction of the Pt(III) species in Step II is also much easier than that of the Pt(IV) species in Step I; the extent of potential inversion is predicted to be 596 and 564 mV for **2** and **3**, respectively. Thus, our calculations suggest that a single two-electron reduction should be observed, in good agreement with experiments shown in Figure 1.

The simplistic interpretation of the computed energies above assumes Nernstian behavior for the redox couples; the various redox intermediates in different oxidation states carrying different numbers of ligands are assumed to establish an equilibrium that follows Boltzmann statistics, and the population of each redox-state is determined by the thermodynamics of these intermediates. In this scenario the voltage at the electrode provides the electrochemical driving force that modulates that redox equilibrium. Whereas these considerations are helpful and familiar from standard electrochemical studies of reversible two-electron reactions, the irreversibility of the underlying chemical events necessitates a significant modification of how the two-electron redox chemistry is treated, as will be discussed below. The timing of the electrochemical and chemical steps is important for understanding the overall redox reaction. The electrochemical and chemical components of the first reduction may occur in a concerted fashion at a reduction potential $E_{1,c}^\circ$ or in a stepwise manner at a different reduction potential $E_{1,s}^\circ$, as conceptualized in Scheme 2. The five-coordinate Pt(III) intermediate is

Scheme 2

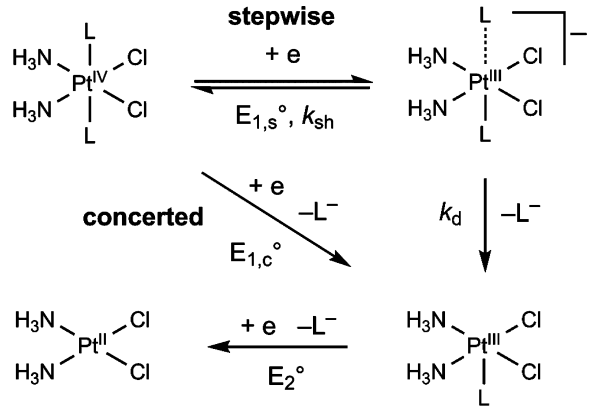

then reduced by transfer of a second electron and loss of a second axial ligand to generate the four-coordinate Pt(II) species at a second reduction potential E_2° via an irreversible overall two-electron transfer (i.e., $E_2^\circ \gg E_{1,c}^\circ/E_{1,s}^\circ$). Our calculations indicate that loss of the second ligand from Pt(III) (Step II-c, Scheme 1) is quite feasible, with the free energy of ligand dissociation being close to zero in all three cases (Table S4 in SI). Hence, the second ligand may dissociate before the second electron transfer occurs. However, it is experimentally impossible to determine if this is so, because the initial process of coupled electron transfer and ligand dissociation is rate-limiting. Similarly, although our quantum chemical simulations suggest a plausible energetic scenario for the reaction sequence shown in Scheme 2, these calculations do not allow for reliably estimating the rate constants k_{sh} or k_d, as pointed out above. This is frustrating, because these mechanistic details are important for a deeper understanding of the prodrug activation process. Most importantly, we must ascertain whether the initial process of reduction and bond cleavage follows a concerted or stepwise pathway, as discussed above.

Mechanism. The question of whether the process of electron transfer and bond cleavage occurs in a stepwise or concerted manner can be addressed using the theory of dissociative electron transfer developed by Savéant.[39,42,43,46,75] Based on the quadratic activation−driving force relationship of Marcus theory[38,76] the scan-rate-dependent changes in the shape of the electrochemically irreversible voltammetric response can be used to extract mechanistic and thermodynamic information. The methodology has been applied most commonly to organic systems, especially alkyl and aryl halides,[39−42,71] but it should be equally applicable to transition-metal complexes. In the present case there is a question regarding the existence of a six-coordinate Pt(III) intermediate $[Pt^{III}(NH_3)_2Cl_2L_2]^-$ as our calculations show both Pt−L_{axial} bonds to become weakened substantially upon

dx.doi.org/10.1021/ja5029765 | J. Am. Chem. Soc. 2014, 136, 8992−9000

addition of the first electron—a plausible expectation, given the half-filling of the Pt(d_{z^2})–L_{axial} σ-antibonding orbital in this step. However, attractive interactions between the positive Pt(III) center and the departing anions may be strong enough to stabilize the transient intermediate. In organic systems attractive interactions due to van der Waals and/or electrostatic forces between product radical and anionic species were found to afford metastable intermediates;[39,77] stronger interactions are to be expected for our inorganic complexes. It should be noted that Savéant's dissociative electron-transfer analysis is strictly phenomenological; i.e., observation of a stepwise response simply suggests the existence of an intermediate where the fragments are not fully dissociated within the time scale of the electrochemical measurement. Therefore, it is not possible to extract any detail about the force responsible for holding the fragments together or to obtain any structural information about the intermediate. Importantly, the underlying theory does not assume a thermodynamic equilibrium between the redox intermediates, and thus, useful information can be extracted for both Nernstian and non-Nernstian redox reactions.

In a typical cyclic voltammetry experiment of a Nernstian redox system, the observable standard potential E^o of a single two-electron redox reaction is the average of the two inverted single-electron potentials, as the energies of both redox events are absorbed by the equilibrium of different redox intermediates in an adiabatic manner. Non-Nernstian behavior arises from situations where a thermodynamic equilibrium cannot be reached, for example because the rate of ligand reattachment at the given low concentration of that ligand in solution is incompatible with the rates of the purely electrochemical events. Under these diabatic conditions, the observable standard potential for the two-electron chemistry is dominated by the more difficult first reduction associated with E_1^o, and the second more positive reduction potential E_2^o does not change the value of the reduction potential but only adds to the observable current. In other words, to initiate the irreversible two-electron redox reaction that generates the desired Pt(II)-complex from its Pt(IV) precursor, two redox equivalents must be delivered at the energy corresponding to the more negative one-electron potential E_1^o, despite the fact that the second electron is in principle easier to be inserted into the one-electron reduced species. Note that Nernstian systems behave differently and the more positive second reduction potential lowers the required energy for the single two-electron event, as explained above.

Savéant[39,42,43,46] and Maran[75,78−85] have demonstrated that concerted and stepwise electron-transfer processes accompanied by bond cleavage display distinctive scan rate dependencies in a cyclic voltammetry experiment. By studying the scan rate dependence of the position and shape of an electrochemically irreversible response, it is possible not only to determine the mechanism of reduction but also to extract a meaningful value for the standard Pt(IV/III) potential, E_1^o. An important difference between the concerted and stepwise mechanisms is the extent to which the voltammetric peak potential, E_{pc}, is displaced from the formal half-reaction potential ($E_{1,s}^o$ or $E_{1,c}^o$). In the concerted mechanism the Pt–L_{axial} bond(s) are cleaved simultaneously with electron transfer, and the six-coordinate Pt(III) intermediate has no discernible lifetime. The thermodynamic potential of the concerted reaction, $E_{1,c}^o$, is much more positive than the potential of the stepwise reaction, $E_{1,s}^o$, because of the energy associated with cleaving the Pt–L bonds. Moreover, the need to cleave these bonds in conjunction with electron transfer adds greatly to the activation barrier of the redox reaction. Therefore, electron transfer via a concerted mechanism is associated with a much larger overpotential and is observed at a much more negative peak potential than its thermodynamic value, $E_{1,c}^o$.[42,75] In the stepwise mechanism the electrochemical response may be influenced by the kinetics of both the electron transfer reaction (k_{sh}), which may be sluggish because of significant, albeit smaller, inner- and outer-shell reorganization energies, and ligand loss (k_d), which is irreversible and likely rapid. The response is equivalent to a quasi-reversible electron transfer followed by an irreversible chemical reaction, i.e., an E_qC_i mechanism.[86] In the stepwise mechanism, the observed peak potential is not shifted greatly from $E_{1,s}^o$—even for an irreversible reaction—because of the competing effects of slow electron transfer, which shifts E_{pc} in the negative direction, and the following chemical reaction, which shifts E_{pc} in the positive direction. Finally, if this mechanism prevails, we can state with some certainty that electron transfer is decoupled from ligand loss.

A second important difference between stepwise and concerted processes is the magnitude of the electrochemical transfer coefficient, α, and its variation with potential. As predicted by the quadratic nature of Marcus theory, α exhibits the potential dependence defined by eq 4:

$$\alpha = 0.5 + \frac{F}{2\lambda}(E_{app} - E^o) \tag{4}$$

where E_{app} is the effective or applied potential and λ is the reorganization energy. The transfer coefficient is determined experimentally from eq 5:

$$\alpha = \frac{47.4}{\delta E_{pc}(mV)} \tag{5}$$

where δE_{pc} is the voltammetric peak width (eq 6), $E_{pc/2}$ is the potential at the half-height of the peak, and E_{app} is defined by eq 7:

$$\delta E_{pc} = |E_{pc} - E_{pc/2}| \tag{6}$$

$$E_{app} = \left(\frac{E_{pc} + E_{pc/2}}{2}\right) \tag{7}$$

Because the electrode reaction is irreversible, E_{pc}, $E_{pc/2}$, and E_{app} shift in the negative direction, and the voltammetric peak broadens (δE_{pc}) as the scan rate υ is increased. These changes create the potential dependence of α, which is predicted to display a linear dependence on E_{app}.

Reductions occurring by a concerted mechanism have large reorganization energies, λ, predicated by the totality of metal–ligand bond cleavage and large negative overpotentials, which result in values of $E_{app} \ll E_{1,c}^o$. Under these conditions α is significantly smaller than 0.5 (eq 4), indicating that electron transfer occurs simultaneously with the chemical step and is challenged by unfavorable kinetics, i.e. high barriers. Electron-transfer reactions occurring by a stepwise mechanism have smaller reorganization energies, much less negative overpotentials, and smaller barriers. As a result $E_{app} \approx E_{1,s}^o$, and α is close to 0.5. If the chemical step identified by k_d in Scheme 2 is sufficiently rapid, the voltammetric response will be solely under kinetic control of the electron transfer reaction and the voltammetric wave may be shifted to potentials slightly positive

dx.doi.org/10.1021/ja5029765 | J. Am. Chem. Soc. 2014, 136, 8992−9000

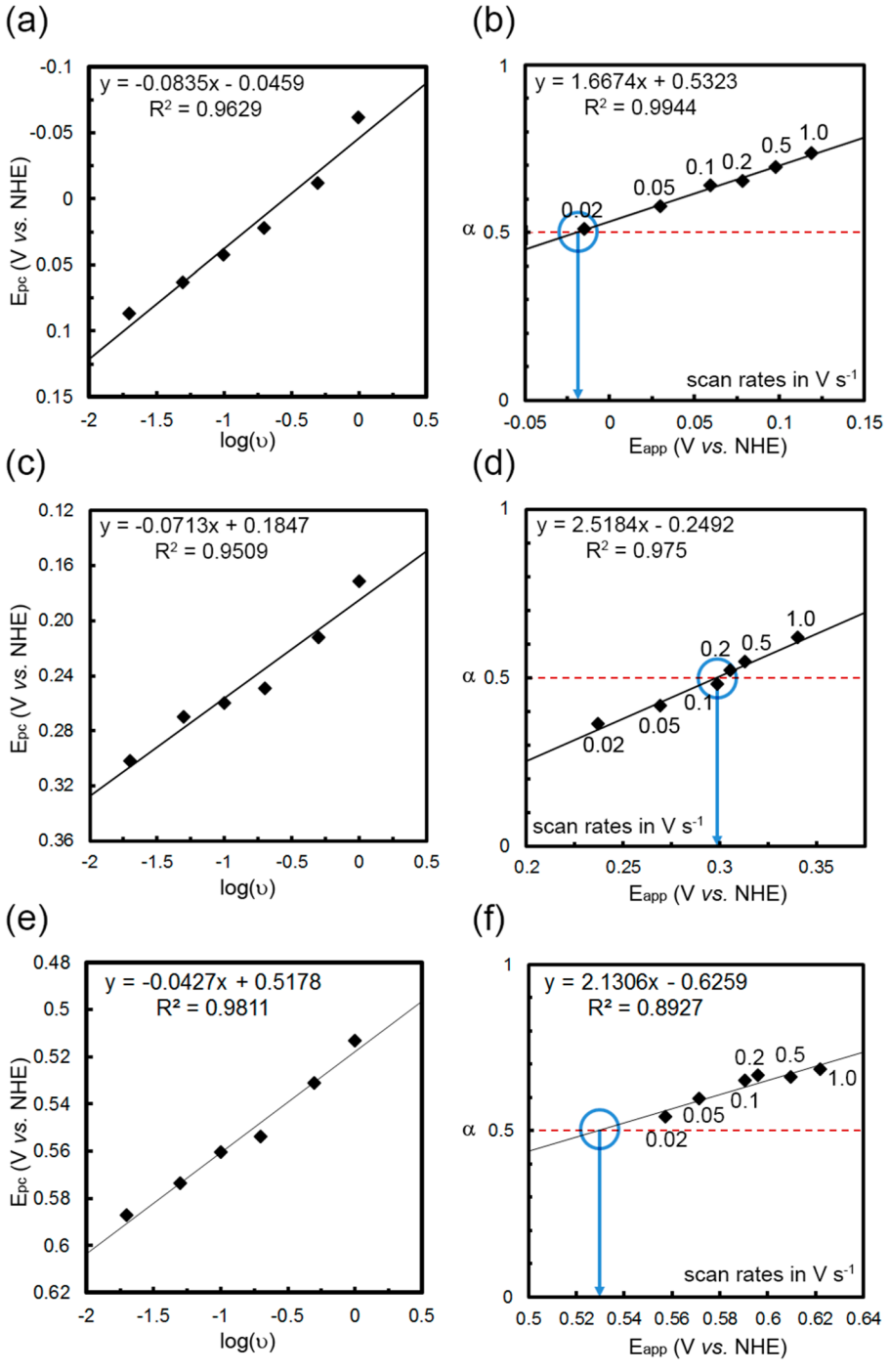

Figure 2. Cathodic peak potentials, E_{pc}, plotted against log of the scan rate, υ, and electron transfer coefficients, α, plotted as a function of E_{app} for **1**, **2**, and **3**.

of $E_{1,s}^{o}$, causing α to exhibit values somewhat greater than 0.5. Figure 2 shows plots of E_{pc} versus log υ and of α versus E_{app} for **1**−**3**. Values of E_{pc} shift in the negative direction with increasing scan rate and exhibit slopes on the order of 40−80 mV per decade consistent with a sluggish electron-transfer reaction followed by a rapid chemical step.[42] The voltammetric waves broaden as scan rate is increased, leading to a slight curvature in the E_{pc}−log υ plots (Figure 2a,c,e) and indicative of Marcus kinetics, which allows α to be plotted as a function of E_{app}.

As shown by Figures 2b,d,f, values of α do not differ greatly from 0.5 and vary linearly with E_{app}. As predicted by eq 4, E_{app} becomes E^{o} when α = 0.5, suggesting estimated standard reduction potentials of −0.019, 0.297, and 0.528 V vs SHE for **1**, **2**, and **3**, respectively.

The relatively narrow range of α values and the fact that they are similar to or slightly larger than 0.5 suggest a stepwise rather than concerted electron-transfer mechanism for the initial reduction of $Pt(NH_3)_2Cl_2L_2$. More specifically, these kinetic parameters are consistent with the six-coordinate Pt(IV) species accepting the first electron to form a six-coordinate Pt(III)-intermediate that exists for a sufficiently long lifetime to impact the reduction potential before the axial ligands dissociate and are lost to the surrounding solvent. As mentioned above, this result is best rationalized by considering

dx.doi.org/10.1021/ja5029765 | J. Am. Chem. Soc. 2014, 136, 8992−9000

that the interactions between the Pt(III) center and the anionic ligands are strong enough such that the departure of the anionic ligands from the Pt(III) center is kinetically inhibited and the overall redox process is pushed toward a stepwise mechanism even when the dative bonds between metal and ligands are considered broken electronically. From our computations alone, we could not have arrived at this insight, as the kinetic protection of the Pt(III)-complex with the acetate ligand bound as an ion pair is challenging to model computationally and is not captured in our simplistic treatment of the thermodynamics for the potential intermediates that uses a continuum solvation model.

Utilizing the conceptual decomposition of electron transfer from Scheme 1 we can now obtain the calculated standard reduction potential for Step I-a, which corresponds to the $E_{1,s}^{\circ}$ value in Scheme 2 for the stepwise reduction of a six-coordinate Pt(IV) to a six-coordinate Pt(III) species. To compare the computed $E_{1,s}^{\circ}$ with the experimental value, the energy from Step I-a is referenced against the standard hydrogen electrode (SHE), the absolute potential of which has been determined in water to be 4.43 V.[87] Thus, the relative potential is computed by use of eq 8:

$$E_{\mathrm{rel}}^{\circ} = -\Delta G(\mathrm{sol}) - 4.43\mathrm{V} \quad (8)$$

For example, **1** has an electron attachment energy of −4.427 eV, so the calculated standard reduction potential from eq 8 is −0.003 V. As shown in Table 2, the experimentally determined standard potential for **1**, −0.019 V, is in excellent agreement with the calculated value with a difference of only 16 mV. For **2**, the computed reduction potential is 0.396 V, which is somewhat more positive than the experimental value of 0.297 but is still in reasonable agreement. Lastly, the potential calculated for complex **3** is 0.451 V, which compares favorably to the experimental potential of 0.528 V. These potentials follow the chemically intuitive expectations; the reduction potential of **2**, which carries the more electron-withdrawing dichloroacetate ligands, is more positive than that of **1**, where the axial ligand positions are occupied by acetato ligands. Complex **3**, the chloro analogue, shows the most positive reduction potential of the three prodrug candidates studied here.

Table 2. Measured versus Computed Standard Reduction Potentials

	experimental (V)			
cmpd	E_{pc} from literature	E_1° from this work	computed (V)	ΔE° (mV)
1	−0.565[36]	−0.019	−0.003	16
2	−0.173[11]	0.297	0.396	99
3	−0.204[36]	0.528	0.451	77

Standard vs Peak Potentials. Previously, several empirical approaches were taken to deduce information about the reduction thermodynamics of various Pt(IV) systems from standard electrochemical measurements. The most common approach is to simply determine the cathodic peak potential E_{pc} of the irreversible cyclic voltammogram at a given scan rate. By keeping the experimental conditions including the scan rate identical, it was assumed that the peak potentials provide a reasonable, semiquantitative measure for the standard reduction potentials. Another popular, anecdotal approach is to record the peak potential shift as a function of the scan rate and extrapolate to a putative potential for the hypothetical scan rate of 0 V s^{-1}. At first sight, these are plausible approaches and are certainly appropriate to obtain qualitative trends in a series of highly related complexes, but the more detailed conceptual analysis that we presented above highlights decisive flaws in these simplistic approaches:

(i) Taking the peak potentials of different complexes at identical scan rates as approximations to the standard reduction potentials implies that the electron-transfer and M−L bond cleavage kinetics are identical in these complexes, i.e. that the peak potential shift as a function of the scan rate for each of these complexes is identical.

(ii) Predicting the peak potential as a close estimate of the standard potential is reasonable for a system that shows reversible, Nernstian redox behavior, as the peak potential is expected to be shifted only by approximately 30 mV (Figure 3). For systems with irreversible or even quasi-reversible behavior, the peak potential will shift from the standard potential by an unpredictable amount, which is representative of the kinetics derived from involvement of slow electron transfer and/or a chemical step.

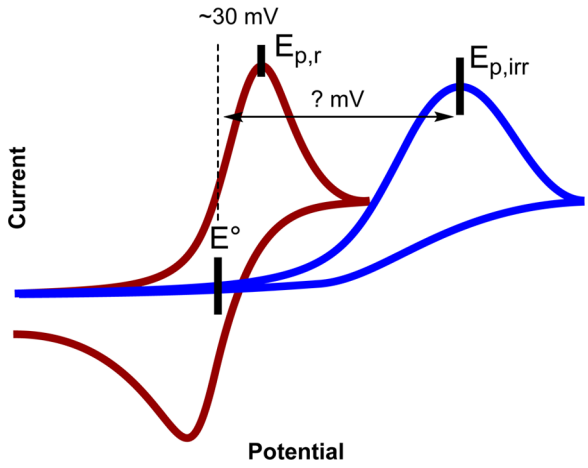

Figure 3. Conceptual comparison of reversible to irreversible peak potentials and how they relate to the standard redox potential.

(iii) Peak potentials can be highly dependent on the type of electrode material employed. Though not entirely predictable, the possibility of a redox-active complex interacting with the chosen electrode material surface must be taken into account. More specifically, the rate of electron transfer from the electrode can drastically change if the redox activity of the complex is affected by the surface structure of the electrode, or if the electrode surface is improperly prepared prior to the CV experiment.[88] In our electrochemical analysis of Pt(IV) prodrugs, metal electrodes such as platinum (Figure 2, Table S5 in SI) and gold (Figure S3, Table S6 in SI) appear to display the most reproducible CV responses required for the Savéant methodology.

Table 2 enumerates the peak potential E_{pc} values previously determined by others.[11,36] Whereas the fact that these are peak potentials and should not be confused with the standard reduction potentials, E°, was widely acknowledged, they have been used synonymously in many chemical interpretations, e.g. to estimate the redox-stability of the prodrug in extracellular medium. The values listed in Table 2 highlight that the peak

dx.doi.org/10.1021/ja5029765 | J. Am. Chem. Soc. 2014, 136, 8992−9000

potentials, −0.565, −0.173, and −0.204 V for **1**, **2**, and **3**, respectively, are consistently more negative than the normal potentials determined in this work. From fundamental considerations, cathodic peak potentials are expected to be more negative than the normal potential; however, the magnitude of the difference enumerated in Table 2 is surprisingly large, which is an illustration of the potential shifting mechanism discussed above.

Finding the accurate standard redox potential is important, because it will determine how these redox-active complexes behave in a biological system, i.e. the extra- and intracellular environments. When the Pt(IV) prodrug interacts with physiologically relevant reducing agents, such as glutathione, in a bimolecular fashion, the overpotential-based shifts of the redox energies become irrelevant and irreversible, diabatic electron transfer occurs within a relatively narrow energy window around the standard potential determined by a Boltzmann statistical distribution. Thus, the standard reduction potential $E_{1,s}^{o}$ is the most relevant measure for estimating the probability of the redox reaction to occur. Utilizing the peak potentials listed in Table 2, which are consistently more negative by as much as 650 mV, leads inevitably to the assumption that the prodrugs **1**−**3** are much more redox-stable than they are in reality. This reasoning may provide an explanation for why the prodrugs tested thus far[89] have displayed much greater redox instabilities than expected. Our combined experimental−theoretical approach to inquiring about the redox properties of non-Nernstian redox couples constitutes a powerful, yet relatively simple, tool for unravelling these convoluted redox chemical events.

CONCLUSIONS

Pt(IV) prodrugs continue to inspire much attention as the next generation of platinum anticancer drugs for the purpose of avoiding the side effects seen commonly from cisplatin; however, the design of these prodrugs appears highly dependent upon the ease of reduction to reach the active Pt(II) analogue. The two-electron redox chemistry of Pt(IV) produgs to their Pt(II) analogues proves to be more complex than previously assumed on the basis of the simple irreversible response from standard electrochemical measurements. A conceptual decomposition of the electron transfer and ligand loss processes with the use of DFT suggests that the addition of an electron to the Pt(III)-complex is much easier than addition to the Pt(IV) analogue. Whereas our quantum chemical simulations provide a reasonable estimate of the energies of the possible redox intermediates, these calculations do not allow for estimating the rate and probability of each step. Whether the electron transfer is coupled to a bond-cleavage event can be determined with the experimental protocol developed by Savéant, as we demonstrated in this work. Concerted and stepwise electron-transfer processes accompanied by bond cleavage display distinctively different scan-rate dependence in a cyclic voltammetry experiment. By studying the differential shapes of the electrochemically irreversible response, not only are we able to determine the mechanism of reduction, but we can also extract a meaningful value for the standard reduction potential of the Pt(IV/III) redox pair that is most important for the redox stability of the prodrug. All Pt(IV) prodrugs **1**−**3** are found to follow a stepwise mechanism for the electron-transfer reaction, where the first addition of an electron affords a six-coordinate Pt(III) intermediate. Although the axial ligand bonds are considered electronically broken, the anionic ligands are still electrostatically attracted to the positively charged Pt-center. As a result, the electron-transfer kinetics is not hindered by a simultaneous chemical step. The standard reduction potentials obtained for all compounds from our Savéant analysis are in excellent agreement with the respective DFT-computed reduction potentials. Our newly determined standard reduction potentials are drastically different from those reported in the literature. Combining results from both experimental and computational approaches, we propose that the electrochemically irreversible Pt(IV)−drug activation is a diabatic, non-Nernstian redox process.

ASSOCIATED CONTENT

Supporting Information

Cartesian coordinates of all complexes, computed energy components, experimental details, CVs, and additional discussion. This material is available free of charge via the Internet at http://pubs.acs.org.

AUTHOR INFORMATION

Corresponding Author

mbaik@indiana.edu

Notes

The authors declare no competing financial interest.

ACKNOWLEDGMENTS

We thank the NSF (CHE-0645381, CHE-1001589 and 0116050) for financial support. M.-H.B. thanks the Research Corporation for the Cottrell Scholarship and the Scialog Award. M.-H.B. thanks Korea University for a WCU Professor appointment. We thank Professor Stephen J. Lippard and his group members for generously providing the Pt(IV)-prodrug compounds.

REFERENCES

(1) Rosenberg, B.; Van Camp, L.; Krigas, T. *Nature* **1965**, *205*, 698.
(2) Rosenberg, B.; Vancamp, L.; Trosko, J. E.; Mansour, V. H. *Nature* **1969**, *222*, 385.
(3) Bosl, G. J.; Motzer, R. J. *N. Engl. J. Med.* **1997**, *337*, 242.
(4) Morris, M.; Eifel, P. J.; Lu, J.; Grigsby, P. W.; Levenback, C.; Stevens, R. E.; Rotman, M.; Gershenson, D. M.; Mutch, D. G. *N. Engl. J. Med.* **1999**, *340*, 1137.
(5) Schiller, J. H.; Harrington, D.; Belani, C. P.; Langer, C.; Sandler, A.; Krook, J.; Zhu, J.; Johnson, D. H. *N. Engl. J. Med.* **2002**, *346*, 92.
(6) Pabla, N.; Dong, Z. *Kidney Int.* **2008**, *73*, 994.
(7) Gregg, R. W.; Molepo, J. M.; Monpetit, V. J.; Mikael, N. Z.; Redmond, D.; Gadia, M.; Stewart, D. J. *J. Clin. Oncol.* **1992**, *10*, 795.
(8) Siddik, Z. H. *Oncogene* **2003**, *22*, 7265.
(9) Zák, F.; Turánek, J. J.; Kroutil, A.; Sova, P.; Mistr, A.; Poulová, A.; Mikolin, P.; Žák, Z.; Kašná, A.; Záluská, D.; Nea, J.; Šindlerová, L.; Kozubík, A. *J. Med. Chem.* **2003**, *47*, 761.
(10) Feazell, R. P.; Nakayama-Ratchford, N.; Dai, H.; Lippard, S. J. *J. Am. Chem. Soc.* **2007**, *129*, 8438.
(11) Dhar, S.; Lippard, S. J. *Proc. Natl. Acad. Sci. U.S.A.* **2009**, *106*, 22199.
(12) Giandomenico, C. M.; Abrams, M. J.; Murrer, B. A.; Vollano, J. F.; Rheinheimer, M. I.; Wyer, S. B.; Bossard, G. E.; Higgins, J. D. *Inorg. Chem.* **1995**, *34*, 1015.
(13) Hall, M. D.; Hambley, T. W. *Coord. Chem. Rev.* **2002**, *232*, 49.
(14) Hall, M. D.; Mellor, H. R.; Callaghan, R.; Hambley, T. W. *J. Med. Chem.* **2007**, *50*, 3403.
(15) Lemma, K.; Berglund, J.; Farrell, N.; Elding, L. I. *J. Biol. Inorg. Chem.* **2000**, *5*, 300.
(16) Dhar, S.; Kolishetti, N.; Lippard, S. J.; Farokhzad, O. C. *Proc. Natl. Acad. Sci. U.S.A.* **2011**, *108*, 1850.

(17) Dhar, S.; Liu, Z.; Thomale, J.; Dai, H.; Lippard, S. J. *J. Am. Chem. Soc.* **2008**, *130*, 11467.
(18) Mantri, Y.; Lippard, S. J.; Baik, M.-H. *J. Am. Chem. Soc.* **2007**, *129*, 5023.
(19) Baik, M.-H.; Friesner, R. A.; Lippard, S. J. *J. Am. Chem. Soc.* **2003**, *125*, 14082.
(20) Jamieson, E. R.; Lippard, S. J. *Chem. Rev.* **1999**, *99*, 2467.
(21) Baik, M.-H.; Friesner, R. A.; Lippard, S. J. *J. Am. Chem. Soc.* **2002**, *124*, 4495.
(22) Wang, D.; Lippard, S. J. *Nat. Rev. Drug Discovery* **2005**, *4*, 307.
(23) Jordan, P.; Carmo-Fonseca, M. *Cell. Mol. Life Sci.* **2000**, *57*, 1229.
(24) Jung, Y.; Lippard, S. J. *Chem. Rev.* **2007**, *107*, 1387.
(25) Wheate, N. J.; Walker, S.; Craig, G. E.; Oun, R. *Dalton Trans.* **2010**, *39*, 8113.
(26) Hartwig, J. F.; Lippard, S. J. *J. Am. Chem. Soc.* **1992**, *114*, 5646.
(27) Chen, L.; Foo Lee, P.; D. Ranford, J.; J. Vittal, J.; Ying Wong, S. *J. Chem. Soc., Dalton Trans.* **1999**, 1209.
(28) Nakai, T.; Ando, M.; Okamoto, Y.; Ueda, K.; Kojima, N. *J. Inorg. Biochem.* **2011**, *105*, 1.
(29) Reithofer, M. R.; Bytzek, A. K.; Valiahdi, S. M.; Kowol, C. R.; Groessl, M.; Hartinger, C. G.; Jakupec, M. A.; Galanski, M.; Keppler, B. K. *J. Inorg. Biochem.* **2011**, *105*, 46.
(30) Platts, J.; Ermondi, G.; Caron, G.; Ravera, M.; Gabano, E.; Gaviglio, L.; Pelosi, G.; Osella, D. *J. Biol. Inorg. Chem.* **2011**, *16*, 361.
(31) Platts, J. A.; Hibbs, D. E.; Hambley, T. W.; Hall, M. D. *J. Med. Chem.* **2000**, *44*, 472.
(32) Ellis, L. E.; HM; Hambley, T. W. *Aust. J. Chem.* **1995**, *48*, 793.
(33) Choi, S.; Filotto, C.; Bisanzo, M.; Delaney, S.; Lagasee, D.; Whitworth, J. L.; Jusko, A.; Li, C.; Wood, N. A.; Willingham, J.; Schwenker, A.; Spaulding, K. *Inorg. Chem.* **1998**, *37*, 2500.
(34) Wilson, J. J.; Lippard, S. J. *Inorg. Chem.* **2011**, *50*, 3103.
(35) Hall, M. D.; Amjadi, S.; Zhang, M.; Beale, P. J.; Hambley, T. W. *J. Inorg. Biochem.* **2004**, *98*, 1614.
(36) Gramatica, P.; Papa, E.; Luini, M.; Monti, E.; Gariboldi, M.; Ravera, M.; Gabano, E.; Gaviglio, L.; Osella, D. *J. Biol. Inorg. Chem.* **2010**, *15*, 1157.
(37) Battle, A. R.; Choi, R.; Hibbs, D. E.; Hambley, T. W. *Inorg. Chem.* **2006**, *45*, 6317.
(38) Marcus, R. A.; Sutin, N. *Biochim. Biophys. Acta* **1985**, *811*, 265.
(39) Costentin, C.; Robert, M.; Savéant, J.-M. *Chem. Phys.* **2006**, *324*, 40.
(40) Savéant, J.-M. *Adv. Phys. Org. Chem.* **2000**, 117.
(41) Savéant, J. M. *J. Phys. Chem.* **1994**, *98*, 3716.
(42) Andrieux, C. P.; Robert, M.; Saeva, F. D.; Savéant, J.-M. *J. Am. Chem. Soc.* **1994**, *116*, 7864.
(43) Savéant, J. M. *Acc. Chem. Res.* **1993**, *26*, 455.
(44) Andrieux, C. P.; Differding, E.; Robert, M.; Savéant, J. M. *J. Am. Chem. Soc.* **1993**, *115*, 6592.
(45) Andrieux, C. P.; Le Gorande, A.; Savéant, J. M. *J. Am. Chem. Soc.* **1992**, *114*, 6892.
(46) Savéant, J. M. *J. Am. Chem. Soc.* **1987**, *109*, 6788.
(47) Savéant, J. M. *J. Am. Chem. Soc.* **1992**, *114*, 10595.
(48) Baik, M.-H.; Ziegler, T.; Schauer, C. K. *J. Am. Chem. Soc.* **2000**, *122*, 9143.
(49) Baik, M.-H.; Friesner, R. A. *J. Phys. Chem. A* **2002**, *106*, 7407.
(50) Baik, M.-H.; Schauer, C. K.; Ziegler, T. *J. Am. Chem. Soc.* **2002**, *124*, 11167.
(51) Ghosh, S.; Baik, M. H. *Inorg. Chem.* **2011**, *50*, 5946.
(52) Lord, R. L.; Schauer, C. K.; Schultz, F. A.; Baik, M. H. *J. Am. Chem. Soc.* **2011**, *133*, 18234.
(53) *Jaguar* 7.0; Schrödinger, Inc.: Portland, OR, 2003.
(54) Becke, A. D. *Phys. Rev. A* **1988**, *38*, 3098.
(55) Becke, A. D. *J. Chem. Phys.* **1993**, *98*, 5648.
(56) Vosko, S. H.; Wilk, L.; Nusair, M. *Can. J. Phys.* **1980**, *58*, 1200.
(57) Lee, C.; Yang, W.; Parr, R. G. *Phys. Rev. B* **1988**, *37*, 785.
(58) Hay, P. J.; Wadt, W. R. *J. Chem. Phys.* **1985**, *82*, 270.
(59) Wadt, W. R.; Hay, P. J. *J. Chem. Phys.* **1985**, *82*, 284.
(60) Dunning, T. H. *J. Chem. Phys.* **1989**, *90*, 1007.
(61) Marten, B.; Kim, K.; Cortis, C.; Friesner, R. A.; Murphy, R. B.; Ringnalda, M. N.; Sitkoff, D.; Honig, B. *J. Phys. Chem.* **1996**, *100*, 11775.
(62) Friedrichs, M.; Zhou, R. H.; Edinger, S. R.; Friesner, R. A. *J. Phys. Chem. B* **1999**, *103*, 3057.
(63) Edinger, S. R.; Cortis, C.; Shenkin, P. S.; Friesner, R. A. *J. Phys. Chem. B* **1997**, *101*, 1190.
(64) Rashin, A. A.; Honig, B. *J. Phys. Chem.* **1985**, *89*, 5588.
(65) Lord, R. L.; Schultz, F. A.; Baik, M.-H. *Inorg. Chem.* **2010**, *49*, 4611.
(66) Evans, D. H. *Chem. Rev.* **2008**, *108*, 2113.
(67) Uhrhammer, D.; Schultz, F. A. *J. Phys. Chem. A* **2002**, *106*, 11630.
(68) Rivada-Wheelaghan, O.; Ortuno, M. A.; Garcia-Garrido, S. E.; Diez, J.; Alonso, P. J.; Lledos, A.; Conejero, S. *Chem. Commun.* **2014**, *50*, 1299.
(69) Bois, H.; G. Connelly, N.; G. Crossley, J.; Guillorit, J.-C.; R. Lewis, G.; Guy Orpen, A.; Thornton, P. *J. Chem. Soc., Dalton Trans.* **1998**, 2833.
(70) Stephen, E.; Blake, A. J.; Davies, E. S.; McMaster, J.; Schroder, M. *Chem. Commun.* **2008**, 5707.
(71) Pandey, K. K. *Coord. Chem. Rev.* **1992**, *121*, 1.
(72) Evans, D. H.; Hu, K. *J. Chem. Soc., Faraday Trans.* **1996**, *92*, 3983.
(73) Evans, D. H. *Acta Chem. Scand.* **1998**, *52*, 194.
(74) Evans, D. H.; Lehmann, M. W. *Acta Chem. Scand.* **1999**, *53*, 765.
(75) Maran, F.; Wayner, D. D. M.; Workentin, M. S. *Adv. Phys. Org. Chem.* **2001**, *36*, 85.
(76) Marcus, R. A. *Annu. Rev. Phys. Chem.* **1964**, *15*, 155.
(77) Wentworth, W. E.; George, R.; Keith, H. *J. Chem. Phys.* **1969**, *51*, 1791.
(78) Antonello, S.; Maran, F. *J. Am. Chem. Soc.* **1997**, *119*, 12595.
(79) Antonello, S.; Musumeci, M.; Wayner, D. D. M.; Maran, F. *J. Am. Chem. Soc.* **1997**, *119*, 9541.
(80) Antonello, S.; Maran, F. *J. Am. Chem. Soc.* **1998**, *120*, 5713.
(81) Antonello, S.; Maran, F. *J. Am. Chem. Soc.* **1999**, *121*, 9668.
(82) Daasbjerg, K.; Jensen, H.; Benassi, R.; Taddei, F.; Antonello, S.; Gennaro, A.; Maran, F. *J. Am. Chem. Soc.* **1999**, *121*, 1750.
(83) Antonello, S.; Crisma, M.; Formaggio, F.; Moretto, A.; Taddei, F.; Toniolo, C.; Maran, F. *J. Am. Chem. Soc.* **2002**, *124*, 11503.
(84) Antonello, S.; Benassi, R.; Gavioli, G.; Taddei, F.; Maran, F. *J. Am. Chem. Soc.* **2002**, *124*, 7529.
(85) Meneses, A. B.; Antonello, S.; Arevalo, M. C.; Gonzalez, C. C.; Sharma, J.; Wallette, A. N.; Workentin, M. S.; Maran, F. *Chem.—Asian J.* **2007**, *13*, 7983.
(86) Evans, D. H. *J. Phys. Chem.* **1972**, *76*, 1160.
(87) Reiss, H.; Heller, A. *J. Phys. Chem.* **1985**, *89*, 4207.
(88) Unpublished results.
(89) Lippard S. J. Personal communication.